AUTHOR'S POST PRINT (Romeo Colour: Green)
Journal of Spacecraft and Rockets (ISSN: 0022-4650), 40 (2): 201-210 (2003).
DOI: 10.2514/2.3954
Publisher version available at
http://www1.aiaa.org/content.cfm?pageid=406&gTable=JaPaperImport&gid=3954

ASSESSMENT OF THE THERMOVIBRATIONAL THEORY: APPLICATION TO G-JITTER ON THE SPACE-STATION

R. Savino‡, M. Lappa*
Università degli Studi di Napoli "Federico II", Dipartimento di Scienza e Ingegneria dello Spazio "Luigi G. Napolitano", P.le V.Tecchio 80, 80125 Napoli (Italy)

This paper deals with the numerical modelling of the effects of g-jitter (oscillatory residual acceleration disturbances) of the type prevailing on the International Space Station. Aim of the work is the extension of the averaging technique, initially introduced by the thermovibrational theory, by evaluating the orders of magnitude of all the terms appearing in the complete equations and identifying the role and the importance of average and periodic terms. The evaluation of the most important terms in the momentum and in the energy equation is made by an "a posteriori" order of magnitude analysis (OMA) by means of the numerical solution of the unsteady full Navier Stokes equations. The discussion of the results identify different regimes and help clarifying some apparent contradictions in the current literature on the effects of g-jitter on temperature disturbances generated by convective motions. The identification of the set of "reduced" equations and associated ranges of validity is of potential great importance for the scientific community. They in fact can be used to obtain analytical and/or mixed numerical/analytical solutions that can lead to a significant reduction of the often prohibitive computational time required for the simulation of the phenomena under investigation.

Introduction

Exploitation of Microgravity Environments in Physical Sciences (Fluid Science, Material Science) is motivated in most cases by the establishment of purely diffusive regimes (i.e. processes that take place in quiescent fluid media) that would prevail in an ideal (zero-g) environment. Typical experiments that would benefit of a quiescent or a quasi-quiescent condition are crystal growth, solidification processes, experiments for the measurement of diffusion or thermodiffusion coefficients, and many others. These experiments are characterized by heat and mass transfer processes in fluid phases in presence of density gradients, caused by thermal gradients (due to heat exchange or to latent heat release during a phase change) or by concentration gradients arising, for example, from the rejection or the incorporation of solute at a solidification interface.
In the presence of accelerations (including steady and periodic accelerations of different amplitudes and frequencies) the velocity, temperature and concentration fields can be determined by the differential balance equations (for mass, momentum, energy and mass species). These accelerations typically induce convective motions that may be important for fluid and material science microgravity experimentation on the International Space Station (ISS), even if the residual gravity is reduced by several orders of magnitude and relatively small amplitude g-jitter are present (see e.g. Figs. 1).
Oscillatory g-jitter includes all the periodic time-dependent accelerations that can be approximated by sinusoidal functions. The most common sources of these accelerations are structural vibrations (e.g. at the fundamental natural frequencies), equipment operations and crew activity (e.g. repetitive exercises that induce cyclic displacement of the position of the test cell).

‡ Associate Professor of Fluid Dynamics, Department of Space Science and Engineering, Univ. of Naples "Federico II", Pzz.le Tecchio 80, 80125, Naples, Italy, E-mail: rasavino@unina.it
* PhD, Research Scientist, address as above, current e-mail address: marcello.lappa@strath.ac.uk

The behaviour of fluid systems subject to sinusoidal accelerations has been the subject of intensive research in the last decade. Many theoretical and numerical studies have been dedicated to this topic[1-6].
It has been shown by an extensive numerical experimentation[7-11] that when soliciting the fluid cell by periodic accelerations, the diffusive temperature distribution $T_d(\underline{r},t)$ and/or the concentration distribution $c_d(\underline{r},t)$ are distorted and the difference (suitably defined) between the temperature (and/or concentration) distribution and the diffusive (ideal) one, can define the g-jitter "disturbance" (if this disturbance exceeds some threshold values, one may say that the Microgravity Environment of the platform is not "tolerable" by the experiment).
In particular, a number of computations for different study cases pointed out that the velocity field **V**, induced by periodic **g** is made up by an average value $\overline{\mathbf{V}}$ plus a periodic oscillation of amplitude $\mathbf{V}'$ ($\mathbf{V} = \overline{\mathbf{V}} + \mathbf{V}'$) at the g-jitter frequency f or at frequencies multiple of f. As a result of the convective field, the scalar quantities (temperature and/or species concentration) are also distorted. These distortions are also made up by a steady plus an oscillatory contribution.
Theoretical[1,4,6,7] and numerical results[3,10,12] available in literature pointed out that different situations may occur, depending on the oscillation frequency. Numerical results by Savino and Monti[12] show that, increasing the frequency, there is a first regime characterized by relatively large oscillatory velocity and oscillatory temperature disturbances and relatively small time-average steady disturbances. At high frequencies the oscillatory thermal disturbances are very small with respect to the steady ones induced by the time-average part of the velocity field (see Fig.2a, that will be discussed later). This behaviour suggested the investigators to introduce strong simplifications in the analysis of the disturbances computation. In particular, according to the Gershuni formulation[13] the time-averaged distortions can be simply computed (i.e. with much less computation time) by a simplified set of equations in terms of quantities averaged over the oscillation period.
The present work wants to extend the averaging technique (initially introduced by the thermovibrational theory) that is valid only at the extreme values of small amplitudes of the periodic displacements and high frequencies. The extension is obtained by

evaluating the order of magnitude of all the terms appearing in the complete equations and by identifying the role and the importance of the average and the periodic terms. Even though the results strictly refer to the specific study case (2-D cell, single fluid with high Pr numbers at periodic conditions, see Figs. 1) a number of conclusions can apply to more general cases as will be seen in the following sections of the paper.

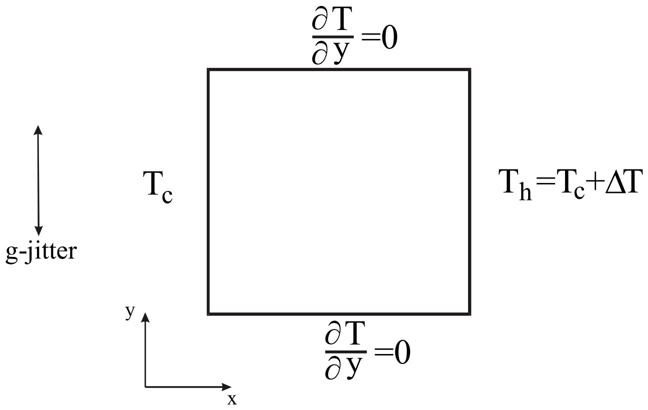

Fig. 1a: sketch of the study case (2-D cell, single fluid with high Pr number at periodic conditions)

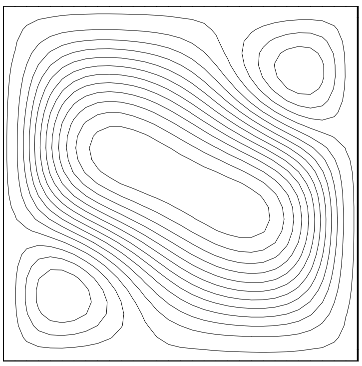

velocity field

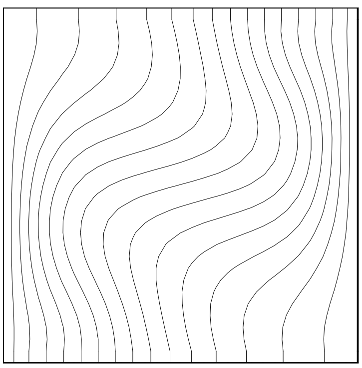

temperature distribution

Fig. 1b. typical flow organization: streamlines and isotherms related to the average flow (Pr=15, $Ra_V = \frac{(b\omega\beta_T \Delta T L)^2}{2\nu\alpha} = 3.3\ 10^4$**)**

The identification of the most important terms in the momentum and in the energy equation will be made with the help of the numerical solution of the unsteady full Navier Stokes equations and will help identifying simplified set of equations (by dropping a number of terms of smaller orders of magnitude) and their range of validity. The proposed methodology is a sort of an "a posteriori" order of magnitude analysis (OMA) that refers to both the full and average Navier-Stokes and energy equations, made on all the terms of the equations. Each variable (T,**V**,p) has been decomposed in the average and oscillatory contribution. The splitting of the variables allows a very detailed OMA that is able to explain the numerical results obtained by different authors.

As mentioned before, for given experimental conditions there is a strong dependence of both types of disturbances (average and periodic) on the g-jitter frequency. Amplitudes of the periodic temperature disturbances tend quickly to decrease with frequency; conversely the average disturbances are less dependent on the frequency so that one expects the unsteady disturbances to "prevail" over the steady ones at low frequencies (and viceversa).

Aim of the present paper is the separation of the steady from the periodic oscillations at the level of the Navier-Stokes equations, to single out what are the terms responsible for the generation of velocity and temperature distribution. In particular we want to: a) generalise the separation between oscillatory and time average difference between the complete solution and the purely diffusive steady state process (T_d); b) identify the leading terms in the equations; c) evaluate the relative importance of each term as function of the frequency.

Note that the identification of set of "reduced" equations and associated ranges of validity is of potential great importance for the scientific community. Simplified set of equations in fact can be used to obtain analytical and/or mixed numerical/analytical solutions of the problem. Regarding this aspect, note that in general the methods attempted by the different investigators to yield these simplified solutions fall into two categories: a) specifying series expansions, substituting them in the partial differential equations and writing simplified algebraic set of equations for the coefficients of the analytical expansions; b) finding some set of alternative equations by mathematical transformation and manipulation of the original set (see e.g. Gershuni et al.[13]). For both cases the probability of success are largely improved by the simplification (by dropping some terms) of the initial set of non-linear equations. By these techniques the solution algorithm can be accelerated up to 100 times with respect to the case of the solution of the complete Navier-stokes equations.

The introduction of these techniques however is out of the scope of the present work and is delayed to forthcoming papers. Here the analysis is restricted to make available for the scientific community the simplified set of equations.

Definition of the disturbances

Let us consider disturbances induced in a fluid cell by a sinusoidal displacement

$$\mathbf{s}(t) = \mathrm{b}\sin\omega \mathrm{t}\ \mathbf{n} \qquad (1)$$

that induces an acceleration:

$$\mathbf{g}(t) = \mathbf{g}_\omega \sin\omega \mathrm{t} \qquad (2)$$

where $\mathbf{g}_\omega = \mathrm{b}\,\omega^2 \mathbf{n}$.

As in most of the cases dealt with in microgravity experimentation, we take the reference conditions to be those prevailing in an ideal 0-g environment that, for most of the experiments, imply quiescent conditions $(\mathbf{V} = \mathbf{0})$ with mass and energy transported only by diffusion. In the following, we will denote by a subscript "d" the parameters corresponding to the purely diffusive conditions (e.g. the temperature T_d (x, y, z, t)). The thermal disturbances induced by any acceleration will therefore be defined at each point (x, y, z) and at any time (t) as:

$$\delta \mathrm{T} = \mathrm{T}\ (\mathrm{x, y, z, t}) - \mathrm{T_d}(\mathrm{x, y, z, t}) \qquad (3)$$

In the case of numerical integration at the grid point "j" of the mesh:

$$\delta T_j(t) = T_j(t) - T_{j_d}(t) \qquad (4)$$

The local temperature can be split into a time averaged steady contribution plus an oscillating part ($T_j = \overline{T}_j + T_j'$) so that the local temperature disturbance reads:

$$\delta T_j = T_j - T_{jd} = \overline{(T_j - T_{jd})} + T_j' \qquad (5)$$

where $\overline{T}_j$ is the non dimensional local temperature averaged over the period $2\pi/\omega$ and T_j' is the oscillatory part expressed in terms of the local amplitude of the temperature oscillation (ΔT_j):

$$T_j' = \Delta T_j \, f_j(\omega) \qquad (6)$$

where $f_j(\omega)$ is a periodic, zero time average function (e.g. = $f_j(\omega) = \sin(\omega t + \varphi_j)$).

In general $\overline{T}_j$ and ΔT_j are function of time until periodic conditions are reached. We will refer to disturbances prevailing in the periodic regime ($t \to \infty$) after an initial transient.

Two different overall thermal disturbance parameters (over all the grid points N) can be defined:

$$\overline{\varepsilon}_T = \frac{1}{N}\sum_{j=1}^{N}\left|\frac{\overline{(T_j - T_{jd})}}{\Delta T}\right| \qquad (7a)$$

$$\varepsilon'_T = \frac{1}{N}\sum_{j=1}^{N}\left|\frac{(\Delta T_j)}{\Delta T}\right| \qquad (7b)$$

Where ΔT is the characteristic temperature difference imposed across the cell (Fig. 1a). The two disturbances parameters are both constant with time at periodic conditions. If both $\overline{\varepsilon}_T$ and ε'_T are <<1, one can assume that the purely diffusive regime is not disturbed by the presence of the on-board acceleration **g**(t).

One can rightly suspect that the two disturbance parameters may play a different role in different processes (e.g. crystal growth, solidification processes, sedimentation) and that no comparison can be made between the two types of disturbances; the order of magnitude of $\overline{\varepsilon}_T$ and ε'_T for the negligibility of the thermal disturbances may be different. This difference is a further reason to evaluate separately the amplitude of the periodic disturbances (in velocity and temperature) related to the angular velocity ω of the forcing g-jitter, and the steady disturbance (again in velocity and temperature) that results from the streaming motion due to the non linear convective terms in the equation.

The analysis that follows will clarify a number of apparent contradictions encountered in the literature on the estimate of the dependence of the temperature (and/or concentration) disturbances on the g-jitter frequency. In fact the results that the disturbances depend on acceleration and frequency as g_ω^2/ω^2 (Monti and Savino[9]) or as g_ω/ω^2 (Monti et al. [1]) are both correct but refer to the two types of disturbances: the first refers to $\overline{\varepsilon}_T$ and the second to ε'_T as shown in Fig. 2b. The different conclusions of the two analyses depend on the different a-priori assumptions made in the momentum and energy equations.

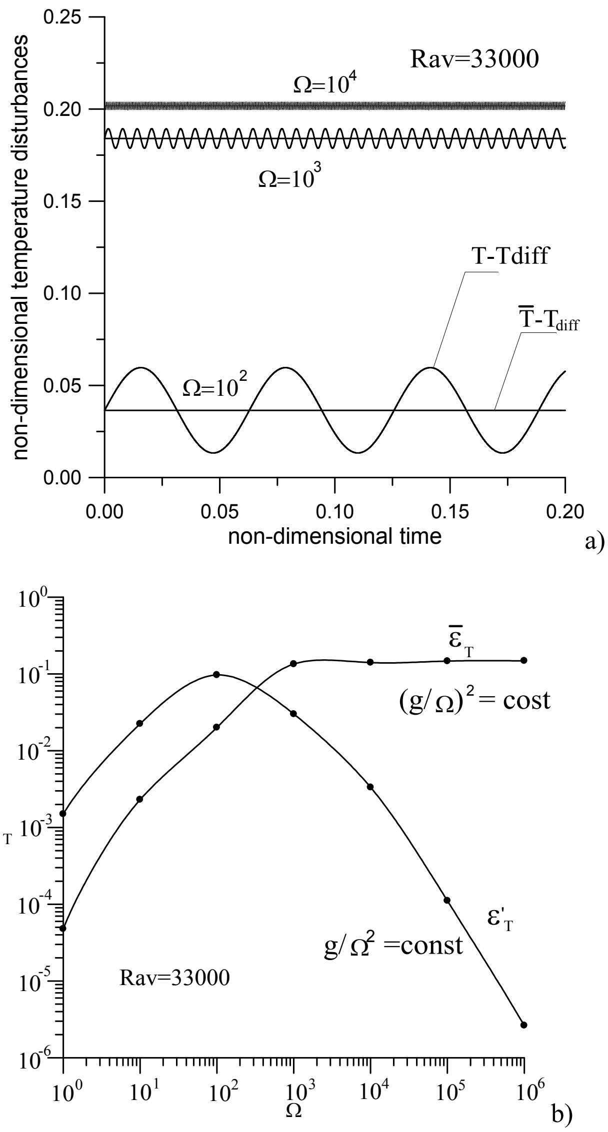

Figs. 2: (a)Non-dimensional temperature in the point x=0.25, y=0.5; (b), disturbances versus Ω ($\Omega = \frac{\omega L^2}{\alpha}$)

In Monti et al.[1] all the non-linear terms were neglected for high values of the frequency. In the Gershuni treatment (as it will be shown later) the non-linear, non-zero time average terms, that are negligible in the momentum and energy equations, are taken into account in the time-average equations to find the time-average velocity and temperature distributions.

Reference case

A 2D test cell with square section of side L in the plane xy is filled with a homogeneous Newtonian liquid (Silicone oil with Kinematic viscosity ν=1 [cs]). All the boundaries of the cavity are solid walls (see Fig. 1a). The walls at x=0 and x=L are maintained at constant temperatures T_c and $T_h = T_c + \Delta T$; the other boundaries are adiabatic. A simple, periodic, sinusoidal acceleration is applied (defined by Eqs. (1) and (2)), characterized by the magnitude g_ω and the direction **n** perpendicular to the imposed temperature gradient.

For the chosen configuration (ΔT= 60 [K], cell size 5x5 [cm^2]) and liquid with Prandtl number Pr=15 (α=6.6 10^{-4} [cm^2/s], β_T= 1.3 10^{-3} [1/K]), the typical flow organization is that shown in Fig. 1b by the streamlines and the isotherms related to the average

flow. A periodic oscillating temperature and velocity field is overimposed to the average field after a sufficient time has elapsed during which constant boundary conditions are maintained.
The relative importance of the temperature periodic oscillations with respect to the steady disturbances ($\bar{T}-T_d$) can be seen in Fig. 2a where the non-dimensional temperature disturbances at a typical field point are reported at different acceleration frequencies. The examples shown refer to three different frequencies proportional to their amplitudes (g_ω/ω=b ω =const). Independent of the magnitude of the steady and pulsating disturbances, the plots intend to show that, for increasing frequencies ($\Omega=\frac{\omega L^2}{\alpha}$), the oscillating part becomes much smaller than the steady part as it will be discussed in details later on.

Numerical solution technique

The flow is governed by the continuity, Navier-Stokes and energy equations, that in dimensional conservative form read :

$$\nabla\cdot\mathbf{V}=0 \qquad (8a)$$

$$\frac{\partial\mathbf{V}}{\partial t}=-\frac{1}{\rho_O}\nabla p-\nabla\cdot[\mathbf{VV}]+\upsilon\nabla^2\mathbf{V}-b\omega^2\beta_T\sin(\omega t)(T-To)\mathbf{n} \qquad (8b)$$

$$\frac{\partial T}{\partial t}=-\nabla\cdot[\mathbf{V}T]+\alpha\nabla^2 T \qquad (8c)$$

where ρ_0 and T_0 relate to reference conditions (e.g. temperature of the cold wall), β_T is the (constant) thermal expansion coefficient ($\beta_T=\frac{1}{\rho}\frac{\partial\rho}{\partial T}$) and **n** is the direction of the acceleration.
From now on we will talk in terms of non dimensional quantities; we denote the non-dimensional T, **V**, p by the same symbols used in Eqs. 8. Equations (8), in non-dimensional form read :

$$\nabla\cdot\mathbf{V}=0 \qquad (9a)$$

$$\frac{\partial\mathbf{V}}{\partial t}=-\nabla p-\nabla\cdot[\mathbf{VV}]+\Pr\ \nabla^2\mathbf{V}-\frac{\Lambda\Omega^2}{\Pr}\sin(\Omega t)T\mathbf{n} \qquad (9b)$$

$$\frac{\partial T}{\partial t}=-\nabla\cdot[\mathbf{V}T]+\nabla^2 T \qquad (9c)$$

where Pr is the Prandtl number (Pr=ν/α). The non-dimensional form results from scaling the co-ordinates by a characteristic length of the problem under investigation (L) and the velocity components (u,v) by the energy diffusion velocity $V_\alpha=\alpha/L$; the scales for the time and the pressure are, respectively, L^2/α and $\rho_o(V_\alpha)^2=\rho_o\alpha^2/L^2$ (α being the thermal diffusivity). The temperature, measured with respect to the reference temperature To (e.g. of the cold wall temperature), is scaled by ΔT. The nondimensional frequency (Ω) and displacement (Λ) are defined by (eqs. 10):

$$\Omega=\frac{\omega L^2}{\alpha}\quad \Lambda=b\frac{\beta_T\Delta T}{L} \qquad (10)$$

At the initial time the liquid filling the cell is supposed to be quiescent and at temperature corresponding to the purely diffusive situation:
t=0: **V**(x, y) = 0 , T_d (x, y)= x (11)
The boundary conditions on the heated walls are the no-slip condition and the temperature conditions:

<u>*on the cold wall*</u>

$$\mathbf{V}\ (x=0,y,t)=0;\ \ T\ (x=0,y,t)=0 \qquad (12a)$$

<u>*on the hot wall*</u>

$$\mathbf{V}\ (x=1,y,t)=0;\ \ T\ (x=1,y,t)=1 \qquad (12b)$$

Equations (9a-9c) subjected to the initial and boundary (Eqs. 11 and 12) conditions were solved numerically in primitive variables by a finite-difference method. The domain was discretized with a uniform mesh and the flow field variables defined over a staggered grid. Forward differences in time and central-differencing schemes in space (second order accurate) were used to discretize the partial differential equations, obtaining:

$$\mathbf{V}^{n+1}=\mathbf{V}^n-\Delta t\nabla p^n+\Delta t\left[-\nabla\cdot(\mathbf{VV})+\Pr\ \nabla^2\mathbf{V}-\frac{\Lambda\Omega^2}{\Pr}\sin(\Omega t)T\ \mathbf{n}\right]^n$$

$$T^{n+1}=T^n+\Delta t\left[-\nabla\cdot(\mathbf{V}T)+\nabla^2 T\right]^n \qquad (14)$$

The computation of the velocity field at each time step has been split into two substeps.
In the first, an approximate velocity field $\mathbf{V}^*$ corresponding to the correct vorticity of the field, but with $\nabla\cdot\mathbf{V}^*\neq 0$, is computed at time (n+1) neglecting the pressure gradient in the momentum equation, i.e.,

$$\mathbf{V}^*=\mathbf{V}^n+\Delta t\left[-\nabla\cdot(\mathbf{VV})+\Pr\ \nabla^2\mathbf{V}-\frac{\Lambda\Omega^2}{\Pr}\sin(\Omega t)T\ \mathbf{n}\right]^n \qquad (15)$$

In the second substep, the pressure field is computed by solving a Poisson equation resulting from the divergence of the momentum equation with the help of the continuity equation:

$$\nabla^2 p^n=\frac{1}{\Delta t}\nabla\cdot\mathbf{V}^* \qquad (16)$$

Finally, the velocity field is updated using the computed pressure field to account for continuity:

$$\mathbf{V}^{n+1}=\mathbf{V}^*-\Delta t\ \nabla p^n \qquad (17)$$

The Poisson equation is solved with a SOR (Successive Over Relaxation) iterative method.
The temperature field at time (n+1) is obtained from eq. (14) after the calculation of the velocity.

Grid refinement study and validation of the code

The numerical prediction of convective instabilities requires a very careful investigation. For this reason the present numerical model has been validated by quantitative comparisons with available numerical results. In particular, in order to check that the code is able to "capture" correctly the effect of periodic acceleration disturbances on the thermofluid-dynamic field, the results obtained solving the complete set of non-linear and time-dependent Navier-Stokes equations (underlying the present numerical algorithm), have been compared with those obtained by Gershuni et al.[13] using their modified set of equations (valid at high frequencies and small amplitude of the disturbance residual acceleration).

A case lying in the range of applicability of the Gershuni formulation has been considered for comparison since: a) the simplified set of Gershuni's equations and associated numerical results represent a robust and reliable example for comparison; b) the simulation of the effect of high frequencies and small amplitude of the acceleration is expected to be the most heavy situation for a code dealing with the numerical solution of the complete equations; in this case, in fact, due to the intrinsic nature of the phenomena (very small oscillation period and amplitude of the disturbance), the numerical prediction of the physics is very delicate and the numerical algorithm has to show high sensitivity and great accuracy.

The comparison has shown that the present results compose very well with those of Gershuni et al.[13] (the simulations agree within 1%). For the sake of brevity the comparison is not shown in detail. For further details see previous works[12] where the same validation was carried out and widely described.

In this sub-section, moreover, in order to show the numerical convergence of the present algorithm a grid refinement study is discussed. The computations have been performed for uniform grids Nx x Ny (the first number denotes the number of collocation points in the x direction, and the second define the grid size in the y direction).

Grid convergence has been obtained for a resolution of 30 x 30 points. However a grid 40x40 has been used for the simulations in order to achieve a very high accuracy of the solution. Note that each simulation has required about 48 hours of computations on a Digital 433 au workstation.

Averaging technique and extension of the analysis

Until now, two methods for g-jitter analysis have been considered in literature: a) numerical computation of the full non-linear and time-dependent Navier-Stokes equations with a time-dependent body force that gives rise to a time-dependent flow; b) numerical solutions of the time-averaged field equations (Gershuni formulation) for the thermovibrational convection problem, obtained under the assumption of sufficiently small amplitudes ($\Lambda<<1$) and sufficiently large frequencies ($\Omega>>1$) of the g-jitter. At these conditions Gershuni and Lyubimov[14] show that, for given Prandtl number, the steady (streaming) convection depends only on one relevant dimensionless parameter, the vibrational Rayleigh number:

$$Ra_V = \frac{(b\omega\beta_T \Delta TL)^2}{2\nu\alpha} = \frac{(\beta_T \Delta TL)^2}{2\nu\alpha}\left(\frac{g}{\omega}\right)^2 = \frac{\Omega^2\Lambda^2}{2\,\mathrm{Pr}} \tag{18}$$

Let us rewrite the Eqs. (9) in terms of the average values $(\overline{\mathbf{V}}, \overline{T})$ plus periodic oscillations $(\mathbf{V}', T')$: $\mathbf{V}=\overline{\mathbf{V}}+\mathbf{V}'$, $T=\overline{T}+T'$.

As a result of this assumption Eqs. (9) can be written as

$$\nabla\cdot\overline{\mathbf{V}} + \nabla\cdot\mathbf{V}' = 0 \tag{19a}$$

$$\frac{\partial\overline{\mathbf{V}}}{\partial t} + \frac{\partial\mathbf{V}'}{\partial t} + \left(\nabla\overline{p} + \nabla p'\right) + \nabla\cdot\left[\overline{\mathbf{V}}\,\overline{\mathbf{V}}\right] + \nabla\cdot\left[\overline{\mathbf{V}}\mathbf{V}'\right] + \nabla\cdot\left[\mathbf{V}'\overline{\mathbf{V}}\right] + \nabla\cdot\left[\mathbf{V}'\mathbf{V}'\right] = \mathrm{Pr}\left(\nabla^2\overline{\mathbf{V}} + \nabla^2\mathbf{V}'\right) - \frac{\Lambda\Omega^2}{\mathrm{Pr}}\sin(\Omega t)\overline{T}\mathbf{n} - \frac{\Lambda\Omega^2}{\mathrm{Pr}}\,T'\sin(\Omega t)\mathbf{n} \tag{19b}$$

$$\frac{\partial\overline{T}}{\partial t} + \frac{\partial T'}{\partial t} + \nabla\cdot\left[\overline{\mathbf{V}}\,\overline{T}\right] + \nabla\cdot\left[\overline{\mathbf{V}}T'\right] + \nabla\cdot\left[\mathbf{V}'\overline{T}\right] + \nabla\cdot\left[\mathbf{V}'T'\right] = \nabla^2\overline{T} + \nabla^2 T' \tag{19c}$$

If the values of **V**(t) and T(t) are known at a given field point, the average values for **V** and T can be computed by:

$$\overline{\mathbf{V}} = \frac{\omega}{2\pi}\int_0^{2\pi/\omega}\mathbf{V}dt, \quad \overline{T} = \frac{\omega}{2\pi}\int_0^{2\pi/\omega}T dt \tag{20}$$

The time dependent parts V' and T' at each instant of time can therefore be defined as:

$$\mathbf{V}' = \mathbf{V} - \overline{\mathbf{V}}, \quad T' = T - \overline{T} \tag{21}$$

Let us assume that periodic conditions are reached:

$$\frac{\partial\overline{\mathbf{V}}}{\partial t} = 0 \text{ and } \frac{\partial\overline{T}}{\partial t} = 0 \tag{22}$$

At these conditions in terms of the following quantities:

$$\boldsymbol{F}_{V1} = \frac{\partial\mathbf{V}'}{\partial t}, \quad \boldsymbol{F}_{V2} = \nabla\overline{p}, \quad \boldsymbol{F}_{V3} = \nabla p',$$
$$\boldsymbol{F}_{V4} = \nabla\cdot\left[\overline{\mathbf{V}}\,\overline{\mathbf{V}}\right], \ \boldsymbol{F}_{V5} = \nabla\cdot\left[\overline{\mathbf{V}}\mathbf{V}'\right], \ \boldsymbol{F}_{V6} = \nabla\cdot\left[\mathbf{V}'\overline{\mathbf{V}}\right],$$
$$\boldsymbol{F}_{V7} = \nabla\cdot\left[\mathbf{V}'\mathbf{V}'\right], \boldsymbol{F}_{V8} = -\mathrm{Pr}\nabla^2\overline{\mathbf{V}}, \boldsymbol{F}_{V9} = -\mathrm{Pr}\nabla^2\mathbf{V}',$$
$$\boldsymbol{F}_{V10} = \frac{\Lambda\Omega^2}{\mathrm{Pr}}\ \sin(\Omega t)\overline{T}\ \mathbf{n},$$
$$\boldsymbol{F}_{V11} = \frac{\Lambda\Omega^2}{\mathrm{Pr}}T'\sin(\Omega t)\mathbf{n} \tag{23a}$$

$$F_{T1} = \frac{\partial T'}{\partial t}, \quad F_{T2} = \nabla\cdot\left[\overline{\mathbf{V}}\,\overline{T}\right], \quad F_{T3} = \nabla\cdot\left[\overline{\mathbf{V}}T'\right],$$
$$F_{T4} = \nabla\cdot\left[\mathbf{V}'\overline{T}\right], \ F_{T5} = \nabla\cdot\left[\mathbf{V}'T'\right], \ F_{T6} = -\nabla^2\overline{T},$$
$$F_{T7} = -\nabla^2 T' \tag{23b}$$

Equations (19b) and (19c) read:

$$\sum_{i=1}^{11}\boldsymbol{F}_{Vi} = 0 \tag{24a}$$

$$\sum_{i=1}^{7}F_{Ti} = 0 \tag{24b}$$

In the above equations, the generic term F_i present in Eqs. (19), can be considered the sum of an average value $\overline{F}_i$(x,y) plus a periodic oscillation F_i' (x,y):

$$\overline{F}_i(x,y)=\frac{\omega}{2\pi}\int_0^{2\pi/\omega}F_i(x,y)dt \quad ; \quad F_i' = F_i - \overline{F}_i \tag{25}$$

By definition $\overline{F_i'} = 0$ so that:

$$\overline{\boldsymbol{F}_{vi}} = \mathbf{0} \text{ for i=1, 3, 5, 6, 9, 10} \tag{26a}$$

$$\overline{F_{Ti}} = 0 \text{ for i=1, 3, 4, 7}$$

and that

$$\boldsymbol{F}_{vi}' = \mathbf{0} \text{ for i=2, 4, 8} \tag{26b}$$

$$F_{Ti}' = 0 \text{ for i=2, 6}$$

Only the non linear periodic oscillating terms, appearing in Eqs. (24), that contain the product of oscillating quantities (F_{v7}, F_{v11}, F_{T5}) have non zero values of the time average:

$$\boldsymbol{F}_{V7} = \overline{\boldsymbol{F}}_{V7} + \boldsymbol{F}_{V7}' \tag{26c}$$

$$\boldsymbol{F}_{V11} = \overline{\boldsymbol{F}}_{V11} + \boldsymbol{F}_{V11}'$$

$$F_{T5} = \overline{F}_{T5} + F_{T5}'$$

When averaging Eqs. (24a) and (24b) one gets:

$$\sum_{i=1}^{11}\overline{\boldsymbol{F}_{Vi}} = 0 \tag{27a}$$

$$\sum_{i=1}^{7}\overline{F_{Ti}} = 0 \tag{27b}$$

then taking into account Eqs. (26a) and (26b), the set for the average balance equations read:

$$\nabla\cdot\overline{\mathbf{V}} = 0 \tag{28a}$$

$$\left(\nabla\overline{p}\right)+\nabla\cdot\left[\overline{\mathbf{V}}\overline{\mathbf{V}}\right]+\nabla\cdot\left[\overline{\mathbf{V}'\mathbf{V}'}\right]= \Pr\left(\nabla^2\overline{\mathbf{V}}\right)-\Lambda\Omega^2/\Pr\ \overline{T'\sin(\Omega t)}\ \mathbf{n} \tag{28b}$$

$$\nabla\cdot\left[\overline{\mathbf{V}}\overline{T}\right]+\nabla\cdot\left[\overline{\mathbf{V}'T'}\right]=\nabla^2\overline{T} \tag{28c}$$

Before going into details of the analysis, let us point out the novelty and the merits of our proposed analysis. The fact that Eqs. (19) show terms containing average and/or oscillating variables allows to perform a more detailed and accurate OMA. Let us take for example the energy equation (19c). A classical approach for the OMA is to estimate (without solving the equations) the order of magnitude of **V**, T and the length scales from which the order of magnitude of each term in the equation can be evaluated.

If we carry on the OMA before separating the average and the oscillating terms, then we are forced either to keep or to neglect terms treating both the oscillatory and the time average components in the same way. On the other hand, once one identifies all the terms one must find a way to estimate both the amplitude of the oscillation and the average values of each variable and then perform a selective" analysis that leads to the identification of negligible terms. What is done in this paper is a sort of "inverse" OMA insofar we have computed the weight of each term after solving the full set of equations. In this way one gets a clear picture of the possibility of neglecting a number of terms instead of others (at different conditions) that very often lead to wrong conclusions as it will be discussed later.

The main goal of the present work is therefore to find the conditions at which some of the terms in Eqs. (19) and Eqs. (28) can be neglected. So one must, first of all, define a procedure for the evaluation, from the numerical solution, of the order of magnitude of each term of the equations at each field point and then to properly average over the entire flow field. The terms $\overline{F_{vi}}$, F_{vi}', $\overline{F_{Ti}}$, F_{Ti}' are computed through the "correct" solution of the full Navier-Stokes equations by evaluating each term at each grid point during the period $2\pi/\omega$. As mentioned before, the analysis is made once periodic conditions are established. The order of magnitude of the zero-average terms is evaluated by computing the maximum ($\mathrm{F}_{\mathrm{i\,max}}$) and the minimum ($\mathrm{F}_{\mathrm{i\,min}}$) during the period $2\pi/\omega$:

$$\Delta\mathrm{F_i}(\mathrm{x,y}) = (\mathrm{F_i}(\mathrm{x,y}))_{\max} - (\mathrm{F_i}(\mathrm{x,y}))_{\min} \tag{29}$$

that represents the amplitude of the oscillatory part of the disturbance $F_i' = \Delta F_i f_i(t)/2$ where $f_i(t)$ is a periodic, zero time average function (e.g. $f_i(t)=\sin(\omega t+\varphi_i)$).

The numerical computation is performed over the N grid points (j=1, N) and overall quantities are defined as:

$$(F_i)_{ov} = \frac{1}{N}\sum_{j=1}^{N}\left|(F_i)_j\right| \tag{30}$$

in particular for the average and oscillatory terms:

$$(\overline{F}_i)_{ov} = \frac{1}{N}\sum_{j=1}^{N}\left|(\overline{F}_i)_j\right| \tag{31a}$$

$$(\Delta F_i)_{ov} = \frac{1}{N}\sum_{j=1}^{N}\left|(\Delta F_i)_j\right| \tag{31b}$$

Numerical analysis for the ISS microgravity environment

We want to find different regimes and different simplified set of equations in the range of Λ and Ω (or Ra_V) of practical interest for typical potential experimentation to be carried out on the International Space Station (ISS). The ISS is characterized by a complex microgravity environment with quasi-steady (residual) g (of the order of magnitude of micro-g) and a g-jitter spectrum g(f) (see Fig.3). Themovibrational theory shows that at high frequency (and small displacements (Ω>>1, Λ<<1) the steady state disturbances increase with the vibrational Rayleigh number. Straight lines corresponding to three values of Ra_V are drawn on the plot of Fig. 3 that cover the range of g(f) to be expected on the ISS and that are above and parallel to the so called "ISS Requirement curve ($Ra_V \cong 3.3\ 10^{-2}$)". Moving along the lines Ra_V =const at increasing frequency one encounters different regimes corresponding to equations with different important terms. The parametric analysis was performed for $10 \le \Omega \le 10^5$ and $10^{-7} \le g_\omega/g_0 \le 10^{-2}$ that correspond to $3.3 \le Ra_V \le 3.3\ 10^4$.

At large Ω, when the steady disturbances prevail over the oscillating ones (see Fig.2), one would expect that, according to the thermovibrational theory, the disturbances stay constant along the lines Ra_V=const. A lower limit of Ω for the validity of the thermovibrational theory (that has been shown to be correct for Ω>>1) and the identification (in terms of Ω) of different regimes for which a simplified set of balance equations apply can be made by comparing the importance of the terms of the equations.

The numerical analysis has been made by solving the complete unsteady Navier-Stokes equations and by computing, a posteriori, each term of the momentum and energy equations for the amplitude of the periodic part and for the averaged ones. All these terms have been plotted versus Ω in the plot of Figs. 4 and 5, for two values of Ra_V (3.3 x10^2 and 3.3 x10^4 that correspond to maximum values to be expected on the International Space Station).

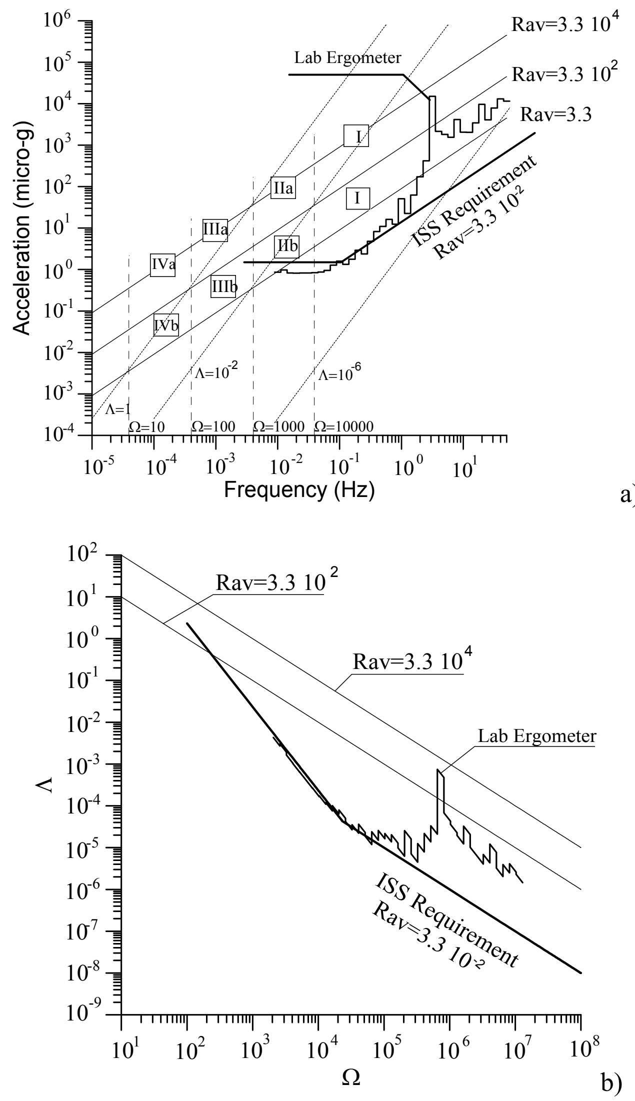

Figs.3: (a),Comparison between predicted accelerations, ISS requirement curve and lines of constant Λ, Ω, Rav in the acceleration-frequency plane; (b), Comparison between predicted accelerations, ISS requirement curve and lines of constant Λ, Ω, Rav in the Λ-Ω plane ($\Omega = \frac{\omega L^2}{\alpha}$, $\Lambda = b\frac{\beta_T \Delta T}{L}$, $Ra_V = \frac{(b\omega\beta_T\Delta TL)^2}{2\nu\alpha} = \frac{(\beta_T\Delta TL)^2}{2\nu\alpha}\left(\frac{g}{\omega}\right)^2 = \frac{\Omega^2\Lambda^2}{2\,\mathrm{Pr}}$ **).**

Comparison of the order of magnitude of each term of the equations is made by plotting the quantities Φ_i' and $\overline{\Phi_i}$ defined by the ratios between each term (i) and the leading term in the momentum (subscript v) and energy (subscript T) equations. In particular

$$\overline{\Phi_{\mathrm{vi}}} = \frac{\left(\overline{\mathrm{F}_{\mathrm{vi}}}\right)_{\mathrm{ov}}}{\left(\Delta \mathrm{F}_{\mathrm{v10}}\right)_{\mathrm{ov}}} \qquad \Phi_{\mathrm{vi}}' = \frac{\left(\Delta \mathrm{F}_{\mathrm{vi}}\right)_{\mathrm{ov}}}{\left(\Delta \mathrm{F}_{\mathrm{v10}}\right)_{\mathrm{ov}}} \tag{32a}$$

$$\overline{\Phi_{\mathrm{Ti}}} = \frac{\left(\overline{\mathrm{F}_{\mathrm{Ti}}}\right)_{\mathrm{ov}}}{\left(\Delta \mathrm{F}_{\mathrm{T4}}\right)_{\mathrm{ov}}} \qquad \Phi_{\mathrm{Ti}}' = \frac{\left(\Delta \mathrm{F}_{\mathrm{Ti}}\right)_{\mathrm{ov}}}{\left(\Delta \mathrm{F}_{\mathrm{T4}}\right)_{\mathrm{ov}}} \tag{32b}$$

where $(\Delta \mathrm{F}_{\mathrm{v10}})_{\mathrm{ov}}$ is the driving term $\mathrm{g}_\omega \beta_\mathrm{T}(\overline{\mathrm{T}} - \mathrm{T}_0)$, and $(\Delta \mathrm{F}_{\mathrm{T4}})_{\mathrm{ov}}$ corresponds to the convective energy transport $\nabla \cdot \left[\mathbf{V}'\overline{T}\right]$.

Analysis of Figs. 4 and 5 shows that the overall relative importance of each term depends on Ω and to a less extent on Ra_V. For instance at very high values of Ω only three terms in the momentum equation (Φ_{v1}', Φ_{v3}', Φ_{v10}') and two terms in the energy equation (Φ_{T1}', Φ_{T2}') (thermovibrational theory) prevail (Regime I).

At the same time, plots of the terms appearing in the averaged momentum and energy equations are shown in Figs. 6 and 7. As a result of the comparison of the different terms, different regimes have been identified. In Appendix the sets of equations for the different regimes for the full and averaged momentum and energy equations are indicated. Separation of the terms in those containing steady and oscillatory contributions shows that in the entire range of Ω and Λ (or Ω and Ra_V) the leading terms in the complete momentum equation is the driving action $\boldsymbol{F}_{v10}' = (\Lambda\Omega^2/\mathrm{Pr})\overline{T}\sin\Omega t\mathbf{n}$ that is almost balanced by the pressure term $\boldsymbol{F}_{v3}' = \nabla p'$. At relatively low frequency the other term to be taken into account is $\boldsymbol{F}_{v9}' = -\mathrm{Pr}\,\nabla^2\mathbf{V}'$ that at $\Omega > 10^4$ can be neglected with respect to the term $\boldsymbol{F}_{v1}' = \frac{\partial \mathbf{V}'}{\partial t}$. In the energy transport equation the two leading terms are $F_{T1}' = \frac{\partial T'}{\partial t}$ and $F_{T4}' = \nabla\cdot\left(\mathbf{V}'\ T\right)$. Unless at very low frequency ($\Omega < 10^2$), in addition a third term must also be taken into account $F_{T7}' = -\nabla^2 T'$. Therefore the full and averaged equations can be summarized as follows:

Full equations

$$\frac{\Lambda\Omega^2}{\mathrm{Pr}}\sin(\Omega t)\overline{T}\mathbf{n} + \nabla p' \begin{cases} = -\mathrm{Pr}\ \ \nabla^2\mathbf{V}' & \text{for } \Omega < 10^3 \\ = \dfrac{\partial \mathbf{V}'}{\partial t} & \text{for } \Omega > 10^3 \end{cases} \tag{33a}$$

$$\frac{\partial T'}{\partial t} + \nabla\cdot\left[\mathbf{V}'\overline{T}\right] \begin{cases} = \nabla^2 T' & \text{for } \Omega < 10^2 \\ = 0 & \text{for } \Omega > 10^3 \end{cases} \tag{33b}$$

Averaged equations

$$\frac{\Lambda\Omega^2}{\mathrm{Pr}}\overline{\sin(\Omega t)T'}\ \mathbf{n} + \nabla\overline{p} - \mathrm{Pr}\ \ \nabla^2\overline{\mathbf{V}} \begin{cases} = 0 & \text{for } \Omega < 10^2 \\ = \nabla\cdot(\overline{\mathbf{V}'\mathbf{V}'}) & \text{for } \Omega > 10^2 \end{cases} \tag{34a}$$

$$\nabla^2\overline{T} \begin{cases} = \nabla\cdot\left[\overline{\mathbf{V}}\overline{T}\right] & \text{for } \Omega > 10^3 \\ = \nabla\cdot\left[\overline{\mathbf{V}'T'}\right] & \text{for } \Omega < 10^3 \end{cases} \tag{34b}$$

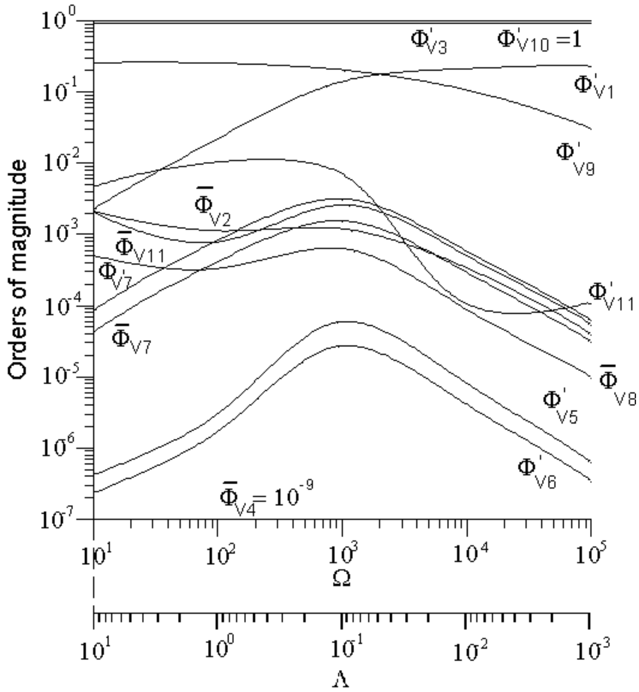

Fig 4a: Comparison between the order of magnitude of the different terms involved in the momentum equation in the case Rav=330 ($\Omega = \frac{\omega L^2}{\alpha}$, $\Lambda = b\frac{\beta_T \Delta T}{L}$, $Ra_V = \frac{\Omega^2 \Lambda^2}{2\Pr}$).

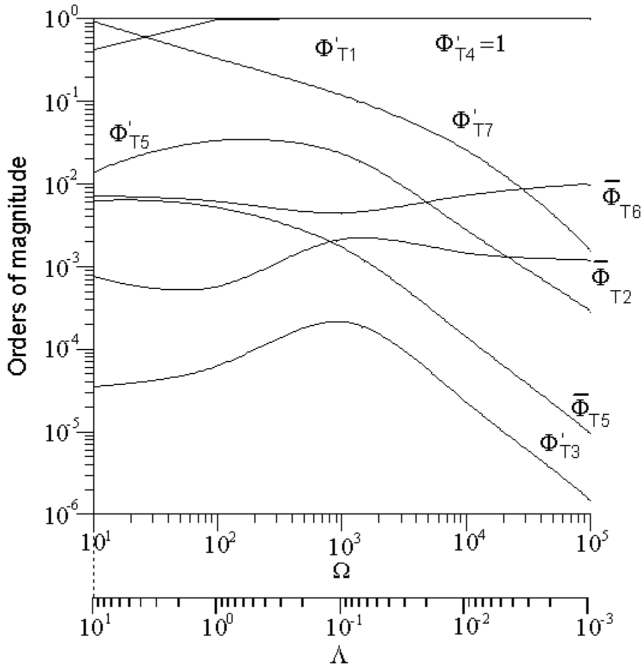

Fig 5a: Comparison between the order of magnitude of the different terms involved in the energy equation in the case Rav=330 ($\Omega = \frac{\omega L^2}{\alpha}$, $\Lambda = b\frac{\beta_T \Delta T}{L}$, $Ra_V = \frac{\Omega^2 \Lambda^2}{2\Pr}$).

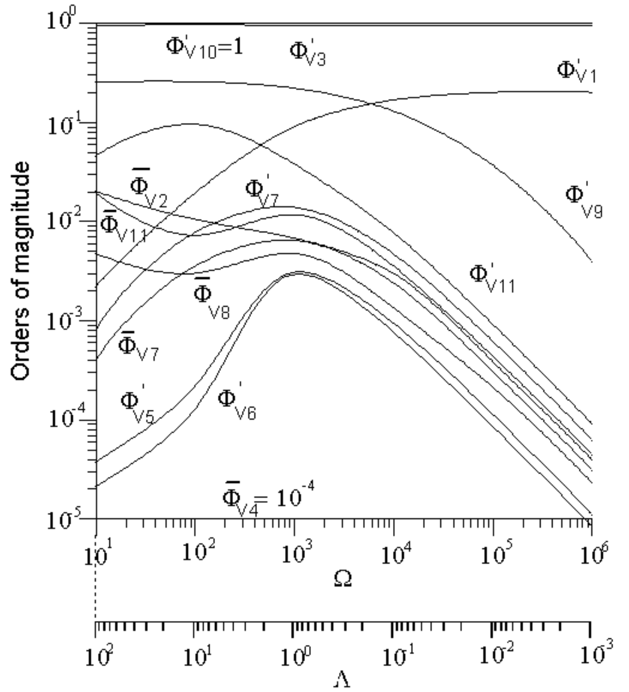

Fig 4b: Comparison between the order of magnitude of the different terms involved in the momentum equation in the case Rav=33000 ($\Omega = \frac{\omega L^2}{\alpha}$, $\Lambda = b\frac{\beta_T \Delta T}{L}$, $Ra_V = \frac{\Omega^2 \Lambda^2}{2\Pr}$).

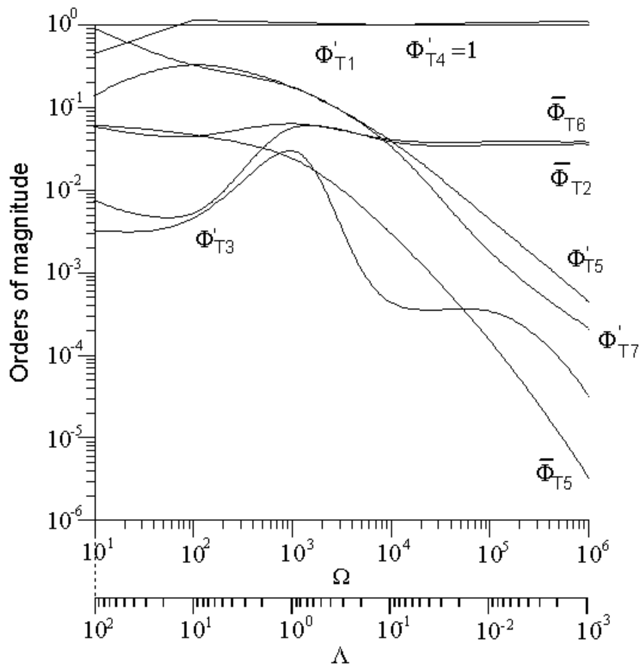

Fig 5b: Comparison between the order of magnitude of the different terms involved in the energy equation in the case Rav=33000 ($\Omega = \frac{\omega L^2}{\alpha}$, $\Lambda = b\frac{\beta_T \Delta T}{L}$, $Ra_V = \frac{\Omega^2 \Lambda^2}{2\Pr}$).

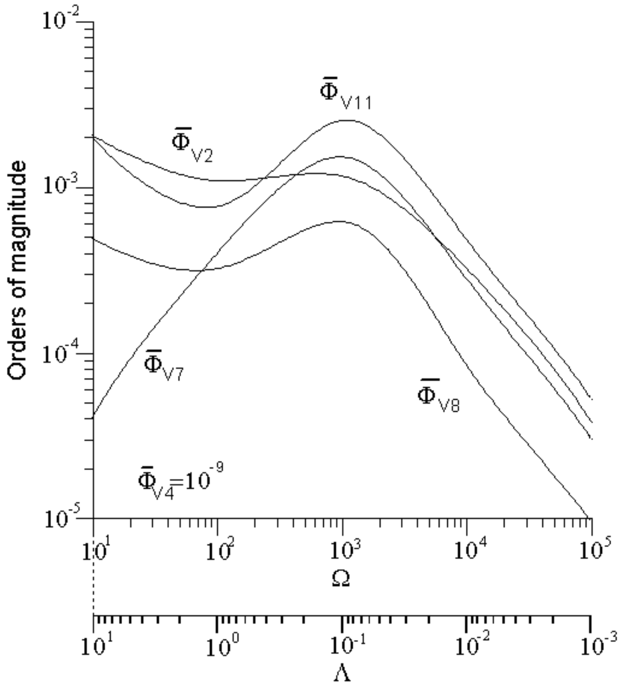

Fig 6a: Comparison between the order of magnitude of the different terms involved in the averaged momentum equation in the case Rav=330 ($\Omega = \frac{\omega L^2}{\alpha}$, $\Lambda = b\frac{\beta_T \Delta T}{L}$, $Ra_V = \frac{\Omega^2 \Lambda^2}{2\Pr}$).

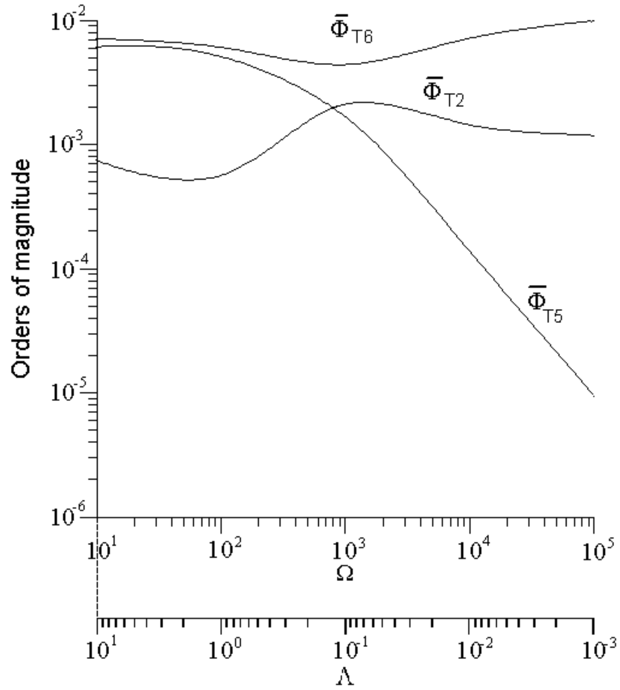

Fig 7a: Comparison between the order of magnitude of the different terms involved in the averaged energy equation in the case Rav=330 ($\Omega = \frac{\omega L^2}{\alpha}$, $\Lambda = b\frac{\beta_T \Delta T}{L}$, $Ra_V = \frac{\Omega^2 \Lambda^2}{2\Pr}$).

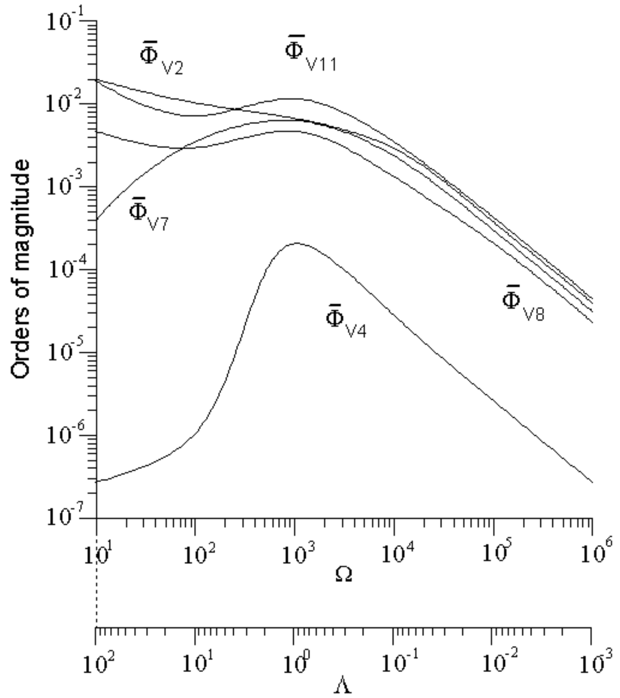

Fig 6b: Comparison between the order of magnitude of the different terms involved in the averaged momentum equation in the case Rav=33000 ($\Omega = \frac{\omega L^2}{\alpha}$, $\Lambda = b\frac{\beta_T \Delta T}{L}$, $Ra_V = \frac{\Omega^2 \Lambda^2}{2\Pr}$).

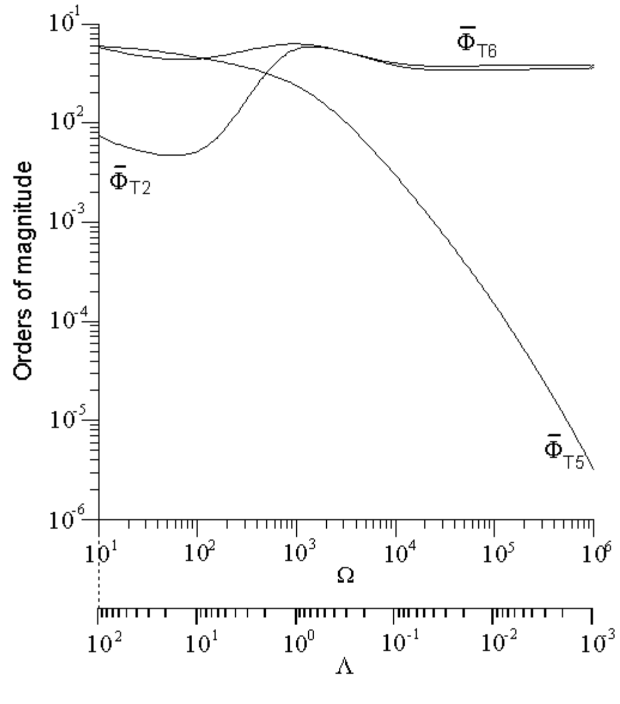

Fig 7b: Comparison between the order of magnitude of the different terms involved in the averaged energy equation in the case Rav=33000 ($\Omega = \frac{\omega L^2}{\alpha}$, $\Lambda = b\frac{\beta_T \Delta T}{L}$, $Ra_V = \frac{\Omega^2 \Lambda^2}{2\Pr}$).

The simplest regime is that corresponding to $\Omega>>1, \Lambda<<1$ (thermovibrational theory) for which approximate relations can be found for **V**' and T' as function of the steady values ($\overline{\mathbf{V}}$, $\overline{T}$) and substituted in the averaged momentum equation where the driving term and the term $\underline{\nabla}\cdot\overline{(\mathbf{V'V'})}$ (that has the same meaning of the turbulence Reynolds stresses) are put together, due to the same dependence on Λ and Ω (see terms $\left(\overline{\Phi_{v11}}\right)$ and $\left(\overline{\Phi_{v7}}\right)$ in Fig. 6 for $\Omega>10^3$).
Intermediate regimes with simplified equations (full and averaged) are indicated in the plot of Figs. 3 and in Appendix.
Order of magnitude analysis can be performed in the limiting cases of very low (quasi steady) or very high frequency. In this last case the analysis yields orders of magnitudes of the disturbances (e.g. thermal disturbances) that depend on the assumptions made on the negligibility of some terms in the momentum and energy equations (in particular the non linear terms related to the forcing action and to the convective terms in the two equations). If all these terms are ignored the disturbance in the system consists of **V**' and T' without average disturbances. When the conditions are such that the non linear terms in the momentum equation are accounted for (i.e. the thermovibrational conditions $\Omega>>1, \Lambda<<1$ prevail), then the viscous term can be neglected, and the main effect of the driving term (with non zero time average) is to generate a streaming or a steady average velocity field that is overimposed to an oscillating velocity field.
Even though all the average terms appearing in the complete equations are of smaller order of magnitude and may appear negligible with respect to the periodic oscillating terms one must consider that the "streaming" steady convective energy transport alters the temperature diffusive distribution more than the oscillating (zero time average) convection.
Indeed it has been shown[12] that at different conditions very small steady residual-g (of the order of few micro-g) generate disturbance effects much larger than the high amplitude g-jitter (because their effects somehow average out over the forcing period).

Evaluation of the thermal disturbances

The two non dimensional disturbances ($\overline{\varepsilon_T}$ and ε'_T) previously introduced have been evaluated for two values of the vibrational Rayleigh numbers (330 and 33330). After reaching the periodic conditions ($\frac{\partial \overline{\mathbf{V}}}{\partial t}=0, \frac{\partial \overline{T}}{\partial t}=0$) time averages of **V** ($\overline{\mathbf{V}}$) and T ($\overline{T}$) are computed by means of the definitions (20).
The value of the difference with the diffusive solution and the temperature oscillation amplitudes are computed at each grid point (j) by the evaluation, in a period, of the average $\overline{T}$ and the difference between the maximum and the minimum. In terms of the non dimensional quantities and of the boundary conditions ($T_{dj}=x_j$), the temperature disturbances at each grid point j read:

$$\overline{T_j}-T_{dj}=\overline{T_j}-x_j \quad (35)$$

$$\Delta T_j=\frac{(T_j)_{\max}-(T_j)_{\min}}{2} \quad (36)$$

from which the two disturbance factors are defined, (see Figs.2);

$$\overline{\varepsilon_T}=\frac{1}{N}\sum_{j=1}^{N}\left(\overline{T_j}-x_j\right)^2; \quad \varepsilon_T'=\frac{1}{N}\sum_{j=1}^{N}\Delta T_j \quad (37)$$

Examination of Fig. 2b shows one of the main results of this study: moving along a curve $Ra_V=(\Lambda^2\Omega^2)/(2Pr)$=const (i.e. along what is assumed today to be the ISS requirement, or the tolerable values of the amplitude of the acceleration versus the acceleration frequency) the value of $\overline{\varepsilon_T}$ tend to level out above say $\Omega=10^3$ (that, for the considered reference case, corresponds to about $4x10^{-3}$ [Hz], see Fig.3); the oscillating disturbance ε'_T rapidly decreases with increasing Ω; for instance at a frequency $f=4x10^{-2}$ [Hz] ($\Omega=10^4$) the value of ε'_T is almost two orders of magnitude lower (at f=4 [Hz] ($\Omega=10^6$) ε'_T is five orders of magnitude lower). Fig. 2b refers to the case Rav=33000. Similar plots are obtained at different Rav with values of the maximum disturbances somehow proportional to Ra_V.
The way the plots of $\overline{\varepsilon_T}$ and ε'_T are constructed (averaging over the period $2\pi/\omega$ and over the whole flow field) suggests that these values can only give an order of magnitude of the overall disturbance; one cannot exclude the possibility that there might be some spots with disturbances higher than the computed ε_T and other points of the field where these disturbances are smaller, if not zero (e.g. at the walls held at constant temperatures). The averaging in time and space, however, is likely to yield overall orders of magnitude that are less dependent on the specific geometry and on the boundary conditions.
A completely different issue is the evaluation of the disturbance effect on different microgravity processes of $\overline{\varepsilon_T}$ and ε'_T; indeed these two factors are not comparable; for instance, even though $\varepsilon'_T<<\overline{\varepsilon_T}$ for experiments that exhibit a high sensitivity to unsteady conditions one may not be in a position to neglect the first type of disturbance with respect to the second one .
The most critical conditions could occur at intermediate Ω where both $\overline{\varepsilon_T}$ and ε'_T are of the same order (albeit less than their maxima). If one follows the ISS requirement curve (g_ω=1[μg] for $\Omega<10^3$; $g_\omega\propto\Omega$ for $\Omega>10^3$) one should expect that indeed in the low frequency part ($Ra_V \propto \Omega^{-2}$) the value of $\varepsilon'_T\cong$const (with negligible $\overline{\varepsilon_T}$) and in the high frequency ($Ra_V\cong$const) $\overline{\varepsilon_T}\cong$const (with negligible ε'_T).
The plot seems to show that the limit transition between g=const to $g\cong\omega$ for ISS specification should be placed at $\Omega\cong10^3$ (see Figs. 3a-3b). Previous works on the tolerability limits (that in the present work correspond to limit values of ε'_T and $\overline{\varepsilon_T}$) apparently show some discrepancies that can be explained on the basis of the above analysis.
The Ref.[1] assumption of the negligibility of the non-linear convective terms with respect to the diffusive terms in both the momentum and energy equations at the high frequencies correctly led to oscillatory disturbance amplitudes in temperature (ε'_T) proportional to g/ω^2 but could not predict steady temperature disturbances. Similarly Naumann[15] neglected the non-linear convective term ($\overline{F_{V7}}$) in the study of the flow in an infinitely long two-dimensional cavity, filled with a fluid subjected to an initial linear temperature distribution.
The present analysis shows that this assumption is not justified in the entire range of frequency and amplitude (for $\Omega>10^3$ and $\Lambda<0.1$ the term $\overline{F_{V7}}$ in the average momentum equation is of the same order of magnitude of the leading terms, see Fig.6). As a result of the assumptions made Naumann[15] found a concentration (or thermal) average disturbance $\overline{\varepsilon_C}$ (or $\overline{\varepsilon_T}$) proportional to g^2/Ω^4 while the present analysis shows that $\overline{\varepsilon_T}$ is proportional to g^2/Ω^2 even though the above mentioned work refers to study cases with different aspect ratios.

Conclusions

The difference and the meaning of the two disturbance parameters $\bar{\varepsilon}$, ε' with respect to the diffusive distributions of scalar quantities (energy and species) have been clarified. The relative importance of the two contributions depend in a different manner on the frequency of the acceleration and (to a less extent) on its amplitude. Previous results available in literature, that seemed to be contradictory, are explained on the recognition that some of them refer to ε' and other refer to $\bar{\varepsilon}$. It is shown that, at low frequencies, the main contributions is given by ε' (that for $\Omega<<1$ refer to quasi steady regimes); at relatively high frequencies ($\Omega>>1$) $\bar{\varepsilon} >> \varepsilon'$ as predicted by the thermovibrational theory. The possibility of evaluating the order of magnitude and the trends of $\bar{\varepsilon}$ and ε' at high Ω has been confirmed for the study case. In the intermediate frequency regimes ($\Omega \cong 10^3$), both $\bar{\varepsilon}$ and ε' have same order of magnitude.
In these regimes one may neglect different terms in the equations; the analysis made suggests different sets of equations obtained by the omission of some terms; the terms that could be omitted have been identified by a detailed analysis made by separating the average from the oscillating part. The risk of omitting non negligible terms may lead to wrong conclusions.
The identification of set of simplified equations and associated ranges of validity can be considered of potential great importance for the scientific community. They in fact can be used to obtain analytical and/or mixed numerical/analytical solutions of the problem that can significantly speed up the simulation of the phenomena under investigation with respect to the case of the solution of the complete Navier-stokes equations.

References

[1]Monti R., Langbein D. and Favier J.J., "Influence of residual accelerations on fluid physics and material science experiments", in Fluid and material Science in Space, H.U. Walter ed., 1987,.

[2]Mc Fadden G.B. and Coriell S.R., "Solutal convection during directional solidification", AIAA Paper 88-3635-CP, 1988.

[3]Schneider S. and Straub J., "Influence of the Prandtl number on laminar natural convection in a cylinder caused by g-jitter", *J. Crystal Growth*, Vol. 46, 1989, pp. 125-131.

[4]Alexander J.I.D., "Low gravity experiment sensitivity to residual acceleration: a review", *Microgravity Sci. and Tech*., Vol. 3, 1990, pp. 52-68.

[5]Ramachandran N., "G-jitter convection in enclosures", *9th International Heat Transfer Conference*, Paper 8-MC-03, August 1990.

[6]Monti R. and Savino R., "The basis and the recent developments of OMA and its applications to microgravity". *Microgravity Quarterly* Vol. 5, N0.1, 1994, pp. 13-17.

[7]Monti R. and Savino R., "A new approach to g-level tolerability for Fluid and Material Science experiments". *Acta Astronautica* Vol. 37, 1994, pp. 313-331.

[8]Monti R. and Savino R., "Influence of g-jitter on fluid physics experimentation on-board the International Space Station". ESA SP-385, 1996, pp. 215-224.

[9]Monti R. and Savino R., "Microgravity experiment acceleration tolerability on space orbiting laboratories". *Journal of Spacecraft and Rockets* Vol. 33, No.5, 1996, pp. 707-716.

[10]Savino R. and Monti R., "Convection induced by residual-g and g-jitters in diffusion experiments". *Int. J. Heat and Mass Transfer* Vol.42, 1999, pp. 111-126.

[11]Savino R. and Monti R., "Improving diffusion controlled microgravity experiments by facility orientation". *Journal of Aerospace Engineering* Vol. 212, Part G, 1999, pp. 415-426.

[12]Savino R. and Monti R. "Fluid dynamic experiment sensitivity to accelerations prevailing on microgravity platforms". In Physics of Fluids in Microgravity *Taylor and Framcis* , 2001.

[13]Gershuni G.Z., Zhukhovitskii E.M. and Yurkov Yu. S., "Vibrational thermal convection in a rectangular cavity", Izv. Akad. Nauk SSSR Mekh. Zhidk. Gaza Vol. 4, 1982, pp. 94-99.

[14]Gershuni G.Z. and Lyubimov D.V., "Thermal Vibrational Convection", John Wiley & Sons, 1998

[15]Naumann R.J., "An analytical model for transport from quasi-steady and periodic accelerations on spacecraft", Int. J. Heat Mass Transfer, Vol. 43, 2000, pp. 2917-2930.

Appendix

The numerical simulation performed for Ω>10000 (Regime I) and Rav=$10^5/3$ show that the simplified set of equation corresponds to the Gershuni ones ($\overline{\Phi}_{V4}$ and $\overline{\Phi}_{T5}$ are negligible in the momentum and in the energy averaged equations respectively; in the complete equations only the terms Φ'_{V1}, Φ'_{V3}, Φ'_{V10}, Φ'_{T1}, Φ'_{T4}, are relevant:

Regime (I)

Complete equations

$$\frac{\partial \mathbf{V}'}{\partial t}+\frac{1}{\rho_O}\nabla p'=b\omega^2\beta_T\ (\overline{T}-To)\sin(\omega t)\mathbf{n} \quad (38a)$$

$$\frac{\partial T'}{\partial t}+\nabla\cdot\left[\mathbf{V}'\overline{T}\right]=0 \quad (38b)$$

Averaged equations

$$\frac{1}{\rho_O}\nabla\overline{p}+\overline{\nabla\cdot\left[\mathbf{V}'\mathbf{V}'\right]}=\nu\nabla^2\overline{\mathbf{V}}+b\omega^2\beta_T\ \overline{T'\sin(\omega t)\mathbf{n}} \quad (38c)$$

$$\nabla\cdot\left[\overline{\mathbf{V}}\overline{T}\right]=\alpha\nabla^2\overline{T} \quad (38d)$$

for 1000< Ω <10000 (Regime IIa) other terms appear in the instantaneous time-dependent flow quantities with respect to the Gershuni formulation; the term Φ'_{V9} , Φ'_{T5} and Φ'_{T7} are no more negligible in the momentum and energy equations respectively. Moreover, the term $\overline{\Phi}_{T5}$ appears in the averaged energy equation.

Regime (IIa)

Complete equations

$$\frac{\partial \mathbf{V}'}{\partial t}+\frac{1}{\rho_O}\nabla p'=b\omega^2\beta_T\ (\overline{T}-To)\sin(\omega t)\underline{n}+\nu\nabla^2\mathbf{V}' \quad (39a)$$

$$\frac{\partial T'}{\partial t}+\nabla\cdot\left[\mathbf{V}'\overline{T}\right]+\nabla\cdot\left[\mathbf{V}'T'\right]=\alpha\nabla^2 T' \quad (39b)$$

Averaged equations

$$\frac{1}{\rho_O}\nabla\overline{p}+\overline{\nabla\cdot\left[\mathbf{V}'\mathbf{V}'\right]}=\nu\nabla^2\overline{\mathbf{V}}+b\omega^2\beta_T\ \overline{T'\sin(\omega t)\mathbf{n}} \quad (39c)$$

$$\nabla\cdot\left[\overline{\mathbf{V}}\overline{T}\right]+\overline{\nabla\cdot\left[\mathbf{V}'T'\right]}=\alpha\nabla^2\overline{T} \quad (39d)$$

for 100< Ω <1000 (Regime IIIa), with respect to the regime IIa, the terms Φ'_{V1} and $\overline{\Phi}_{T2}$ become negligible whereas the terms Φ'_{V11} appears.

Regime (IIIa)

Complete equations

$$\frac{1}{\rho_O}\nabla p'=b\omega^2\beta_T\ (\overline{T}-To)\sin(\omega t)\mathbf{n}+$$
$$b\omega^2\beta_T\ T'\sin(\omega t)\mathbf{n}+\nu\nabla^2\mathbf{V}' \quad (40a)$$

$$\frac{\partial T'}{\partial t}+\nabla\cdot\left[\mathbf{V}'\overline{T}\right]+\nabla\cdot\left[\mathbf{V}'T'\right]=\alpha\nabla^2 T' \quad (40b)$$

Averaged equations

$$\frac{1}{\rho_O}\nabla\overline{p}+\overline{\nabla\cdot\left[\mathbf{V}'\mathbf{V}'\right]}=\nu\nabla^2\overline{\mathbf{V}}+b\omega^2\beta_T\ \overline{T'\sin(\omega t)\mathbf{n}} \quad (40c)$$

$$\overline{\nabla\cdot\left[\mathbf{V}'T'\right]}=\alpha\nabla^2\overline{T} \quad (40d)$$

for 10< Ω <100 (Regime IVa) , with respect to the regime IIIa, the terms Φ'_{T1}, Φ'_{T5} and $\overline{\Phi}_{V7}$ become negligible

Regime (IVa)

Complete equations

$$\frac{1}{\rho_O}\nabla p'=b\omega^2\beta_T\ (\overline{T}-To)\sin(\omega t)\mathbf{n}+$$
$$b\omega^2\beta_T\ T'\sin(\omega t)\mathbf{n}+\nu\nabla^2\mathbf{V}' \quad (41a)$$

$$\nabla\cdot\left[\mathbf{V}'\overline{T}\right]=\alpha\nabla^2 T' \quad (41b)$$

Averaged equations

$$\frac{1}{\rho_O}\nabla\overline{p}=\nu\nabla^2\overline{\mathbf{V}}+b\omega^2\beta_T\ \overline{T'\sin(\omega t)\mathbf{n}} \quad (41c)$$

$$\overline{\nabla\cdot\left[\mathbf{V}'T'\right]}=\alpha\nabla^2\overline{T} \quad (41d)$$

Hereafter the regimes corresponding to Rav=$10^3/3$ are denoted as the (b) regimes:
for Ω >10000 (Regime Ib) the simplified set of equation corresponds to the Gershuni ones as for Rav=$10^5/3$;
for1000< Ω <10000 (Regime IIb), with respect to the regime IIa, the term Φ'_{T5} becomes negligible

Regime (IIb)

Complete equations

$$\frac{\partial \mathbf{V}'}{\partial t}+\frac{1}{\rho_O}\nabla p' = b\omega^2\beta_T\ (\overline{T}-To)\sin(\omega t)\mathbf{n}+\nu\nabla^2\mathbf{V}' \quad (42a)$$

$$\frac{\partial T'}{\partial t}+\nabla\cdot\left[\mathbf{V}'\overline{T}\right]=\alpha\nabla^2 T' \quad (42b)$$

Averaged equations

$$\frac{1}{\rho_O}\nabla\overline{p}+\overline{\nabla\cdot[\mathbf{V}'\mathbf{V}']}=\nu\nabla^2\underline{\overline{V}}+b\omega^2\beta_T\ \overline{T'\sin(\omega t)}\mathbf{n} \quad (42c)$$

$$\nabla\cdot\left[\overline{\mathbf{V}}\overline{T}\right]+\overline{\nabla\cdot[\mathbf{V}'T']}=\alpha\nabla^2\overline{T} \quad (42d)$$

for 100< Ω <1000 (Regime IIIb), with respect to the regime IIIa, the term Φ'_{V11} disappears

Regime (IIIb)

Complete equations

$$\frac{1}{\rho_O}\nabla p' = b\omega^2\beta_T\ (\overline{T}-To)\sin(\omega t)\mathbf{n}+\nu\nabla^2\mathbf{V}' \quad (43a)$$

$$\frac{\partial T'}{\partial t}+\nabla\cdot\left[\mathbf{V}'\overline{T}\right]+\nabla\cdot\left[\mathbf{V}'T'\right]=\alpha\nabla^2 T' \quad (43b)$$

Averaged equations

$$\frac{1}{\rho_O}\nabla\overline{p}+\overline{\nabla\cdot[\mathbf{V}'\mathbf{V}']}=\nu\nabla^2\overline{\mathbf{V}}+b\omega^2\beta_T\ \overline{T'\sin(\omega t)}\mathbf{n} \quad (43c)$$

$$\overline{\nabla\cdot[\mathbf{V}'T']}=\alpha\nabla^2\overline{T} \quad (43d)$$

for 10< Ω <100 (Regime IVb), with respect to the regime IVa, the term Φ'_{V11} disappears

Regime (IVb)

Complete equations

$$\frac{1}{\rho_O}\nabla p' = b\omega^2\beta_T\ (\overline{T}-To)\sin(\omega t)\mathbf{n}+\nu\nabla^2\mathbf{V}' \quad (44a)$$

$$\nabla\cdot\left[\mathbf{V}'\overline{T}\right]=\alpha\nabla^2 T' \quad (44b)$$

Averaged equations

$$\frac{1}{\rho_O}\nabla\overline{p}=\nu\nabla^2\overline{\mathbf{V}}+b\omega^2\beta_T\ \overline{T'\sin(\omega t)}\mathbf{n} \quad (44c)$$

$$\overline{\nabla\cdot[\mathbf{V}'T']}=\alpha\nabla^2\overline{T} \quad (44d)$$